Sensors and Actuators A 203 (2013) 421–429

Contents lists available at ScienceDirect

Sensors and Actuators A: Physical

journal homepage: www.elsevier.com/locate/sna

Robot fingertip tactile sensing module with a 3D-curved shape using molding technique

Dong-Ki Kim [a], Jong-Ho Kim [a,*], Young-Tae Kim [b], Min-Seok Kim [a], Yon-Kyu Park [a], Young-Ha Kwon [b]

[a] Korea Research Institute of Standards and Science, 267 Gajeong-ro Yuseong-gu, Daejeon 305-340, Republic of Korea
[b] Department of Mechanical Engineering, Kyung-Hee University, 1732 Deogyeong-daero, Giheung-gu, Yongin-si, Gyeonggi-do 446-701, Republic of Korea

ARTICLE INFO

Article history:
Received 4 June 2013
Received in revised form
11 September 2013
Accepted 13 September 2013
Available online 29 September 2013

Keywords:
Distributed tactile sensor
Contact-resistance tactile sensor
Robot fingertip
Molding technique
3D-curved surface

ABSTRACT

This paper presents the research findings on a new robot fingertip tactile sensing module, and its simple production method. The module has a three-dimensional curved shape and a radius of curvature of about 7 mm similar to that of human fingertip. The size of the module is 16.3 mm in depth, 16.6 mm in width, and 38 mm in height. A thin and flexible sensing part consists of strip-type force sensors with 37 taxels based on a contact-resistance principle. Each cell is 2 mm in diameter. The force sensors are evaluated through a calibration setup in order to obtain a static force response. The fatigue test is also carried out to check its durability. The 3D-curved fingertip structure is fabricated by the molding technique known as an effective method for mass production. The force sensing part is inserted into the molded fingertip structure. The assembled robot fingertip module is evaluated through a calibration setup in order to obtain the static and dynamic force responses. The fabricated module can detect both contact force and location simultaneously. The threshold sensitivity of one taxel is about 0.2 N. The developed sensing module is compact and replaceable, and its fabrication process is easy and economical.

1. Introduction

Personal robots, such as service robots and entertainment robots, have been developed widely in terms of human–robot interaction. The famous pet robot, AIBO, designed and manufactured by SONY, perceives touch through capacitive touch sensors on its body and head parts for interaction with human [1]. Iwata et al. have tried to attach the film type distributed force sensor to the surface of robot such as shoulder, arm and elbow for human–robot interaction [2]. As the field of robots is continuously expanding to more various environments such as offices, hospitals, homes, and even space, robots are increasingly required to perform advanced human-like manipulation tasks such as shape recognition of objects and grasping objects. In order to achieve advanced in-hand manipulation tasks, many tactile sensors and tactile sensing systems have been reported in various fields of applications [3–4]; a biomedical [5,6], human–robot interaction [7], and dexterous robotic hands [8]. Kinoshita et al. have proposed a shape recognition system with piezo-electric force sensors when their robot hand grasps objects of various shapes [9]. Mouri et al. have used the information about the center of contact points through the distributed force sensor for the grasping task [10]. On the other hand, many studies have reported the distributed force sensor using a variety of sensing methods (e.g., resistive [11–13], capacitive [14,15], piezoresistive [16], piezoelectric [17–19], etc.). Yang et al. have reported a tactile sensing array using flexible PI-copper films [20]. Tekscan Inc. [21] and Interlink Electronics, Inc. [22] have commercialized their film-type contact-resistance force sensors. They are flexible and thin. However, it is difficult to integrate the film type force sensors to the curved structure such as head, arm and hand. Especially, it is much more difficult to apply to fingertip shape because it has very small radius of curvature. Hence, a fabrication technique is required to develop a compact tactile sensing module that can cope with various curved structures.

In our previous work [23], we have proposed the design and the fabrication process of a robot fingertip module that senses both force and location simultaneously. The module has a human fingertip-like shape with a radius of curvature of about 7 mm. The 3D-curved fingertip structure is fabricated by a molding technique known as an inexpensive method in terms of mass production. The contact-resistance type force sensor can obtain only normal force component. It is important to detect the slip information between finger and object in case of grasping task. The slip information can be extracted indirectly by tracking the change of a center of the contact points obtained from the distributed force sensors [24]. The designed sensor has 7×7 strip-type structure in order to insert

* Corresponding author. Tel.: +82 42 868 5241.
E-mail address: jhk@kriss.re.kr (J.-H. Kim).

0924-4247/$ – see front matter © 2013 Published by Elsevier B.V.
http://dx.doi.org/10.1016/j.sna.2013.09.013

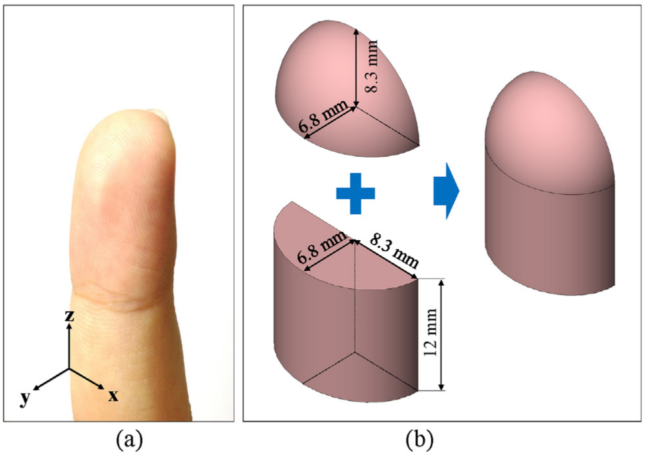

Fig. 1. Design concept for 3D-curved robot fingertip that has human fingertip-like scale and shape: (a) photograph of real human fingertip, and (b) scales of a sensing area that has hybrid structure of elliptic curves for robot fingertip.

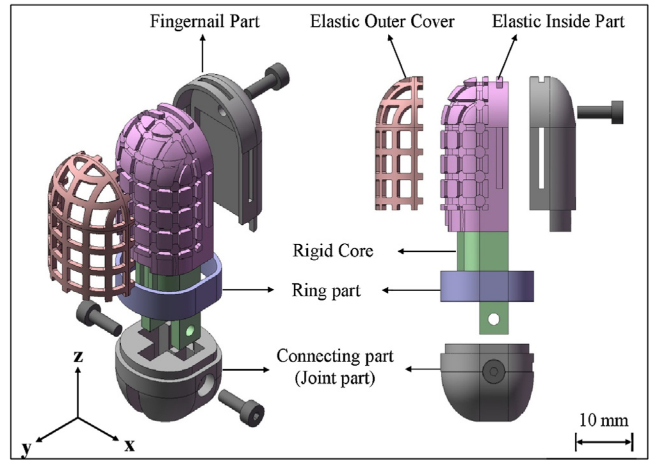

Fig. 2. Three-dimensional (3D) computer-aided design (CAD) of robot fingertip tactile sensing module.

into the fingertip structure. However, the previous work did not show the force response near top area of the fingertip because of a location mismatch of the strip-type force sensor and the molded structure. In this paper, we modified the shape of the strip-type force sensor to match with the fingertip structure and presented the static and dynamic evaluations of the film-type distributed force sensor through the calibration setup. This paper also shows the high cycle fatigue test in order to check its durability and reliability. In addition, the static and dynamic force responses are also obtained using jigs when the distributed force sensor is assembled to the 3D-curved fingertip structure.

2. Design of robot fingertip module

2.1. Design of 3D-curved fingertip structure

Fig. 1 shows the 3D-shape design for robot fingertip that has a human-fingertip-like scale and shape. Fig. 1(a) is a photograph of a real human fingertip. Fig. 1(b) presents the scale of the sensing area of robot fingertip. 3D-curved structure has two different elliptic structures. The lower structure is semi-elliptic cylindrical structure with 8.3 mm in semi-major axis and 6.8 mm in semi-minor axis. Its height is 12 mm from the bottom. The upper structure has two semi-elliptic curves: the one is 8.3 mm in semi-major axis (*z*-axis) and 6.8 mm in semi-minor axis (*x*-axis). Fig. 2 shows the 3D design of the robot fingertip module using SolidWarks^{TM} (Dassault Systemes SolidWarks Co.), 3D CAD software. The designed fingertip is 16.3 mm in depth (*y*-axis direction), 16.6 mm in width (*x*-axis direction), and 38 mm in height (*z*-axis direction), and has a three-dimensional curved shape. The fingertip apparatus consists of the elastic outer-cover, the elastic inside part, a finger-nail part, a ring part, a rigid-core, and a connecting part. The elastic inside part has 7×7 slots like groove for inserting of strip-type thin film sensor and its alignment. The distance between two slots is about 4 mm. The width of the slot is 1 mm, and the depth is 0.8 mm. The elastic outer cover is designed it has a mesh structure to cover the sensing part with force sensors. It has the same outside radius of curvature as the elastic inside part. The width of the mesh is 1 mm, and the thickness of the mesh is 0.8 mm. The rigid-core supports the fingertip structure just as the human bones do. The elastic outer cover and the inside part are fixed by the fingernail part and the ring part. The rigid-core, the fingernail part, and the ring part not only fix the elastic inside part and outer cover but also combine the two. The connecting part links the designed robot fingertip module to various robot hands and grippers. Its design shape depends on the shapes of a target robot-hand [25]. In reference, Schmitz et al. have also tried to apply the capacitive pressure sensor to their finger-tip tactile sensing module for the humanoid robot [26]. It is not easy to obtain the high spatial resolution compared to our 3D-fingertip module with radius of curvature of about 7 mm. Loeb et al. have developed a commercial biomimetic finger-shaped sensor module (BioTAC® [27]). It can detect the contact forces and micro-vibrations [28]. However, the fabrication process is not simple because of the conductive fluid between sensing electrodes and elastomeric skin, and it is not cost-effective. The spatial resolution is also not high compared to our fingertip module.

2.2. Design of the force sensing part

Fig. 3 depicts the computer-aided design (CAD) of the sensing part. The location and distance of each taxel on the 3D surface are needed to place each taxel into the slot of 3D-shaped elastic inside part exactly. We calculated the locations using a mathematical tool, Mathmatica® software. On the other hand, Dahiya et al. have introduced an easy technique that can project 3D structure onto 2D plane and place the sensors on 2D surface, and then reconstruct the same to 3D surface [3]. This technique will be useful to obtain the exact location of each taxel. The designed sensing part

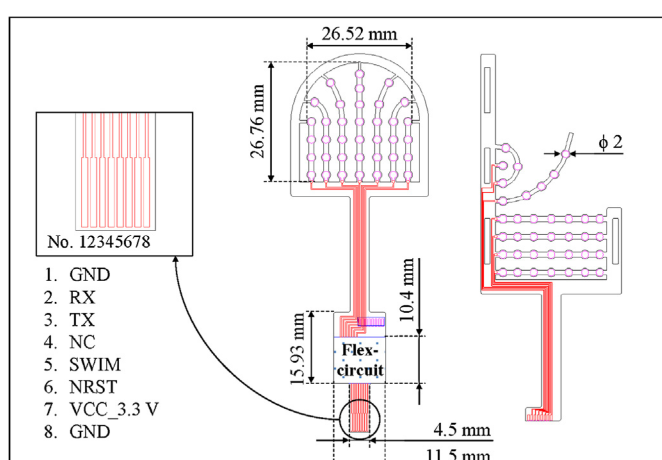

Fig. 3. Computer-aided design (CAD) for the sensing part that consists of a contact-resistance force sensors and the flexible electric circuit board: (left) eight port for data communication; (middle) bottom layer of the force sensors and the flex-circuit for signal processing; (right) top layer of the force sensors.

consists of the contact-resistance type force sensors and the flexible electric circuit board for data signal processing. The force sensor has some advantages: it is flexible and thin because it can be fabricated on a flexible and thin film; it is electrically robust because of its high signal-to-noise ratio; and it is economical because its fabrication process is very simple and easy. The sensing part should be thin, flexible and strip-type in order to insert into the 3D-curved robot fingertip structure [29]. The designed sensing part has 37 taxels, and each taxel is 2 mm in diameter. Although the distributed force sensor is 7×7 matrix structure, it has 37 taxels due to the double-curved shape of the robot fingertip structure. In case of human being's fingertip, the spatial resolution is about 1-2 mm [4,30]. It is important to increase the total number of taxels within the 3D-curvered fingertip structure in terms of more exact contact information. We determined the size of taxels and the spatial resolution considering the size of the used commercial chip and its total number of ports. Each taxel is uniformly distributed at fingertip structure. Especially, some taxels are located at tip area of the fingertip for an effective grasping task. Spatial resolution of the distributed force sensor is about 4 mm. It seems that the number of sensing elements is small, and the spatial resolution is low. However, the spatial resolution can be higher because it is possible to fabricate the force sensor with size of about 1 mm in diameter. The contact-resistance force sensor should have both upper and lower resistive layers for measuring the change of resistance under contact force. The contact-resistance between the two layers changes when the upper layer is subjected to an external load. The middle image of the Fig. 3 shows the design of the bottom layer of the distributed force sensor and the flexible circuit board. The right image presents the design of the top layer of the force sensor. The left image describes an eight electric port of the flexible circuit board for data communication: the port numbers 1 and 8 are for ground; the port numbers 2 and 3 are used for data transmission between the sensor and the computer; the ports 5 and 6 are used to upload a program from the computer to a chip on the circuit board; the port 4 is used for the interrupt mode; and the port 7 is used to apply operating voltage (3.3 V) for the chip and circuit. Thus, only four ports, ports 2, 3, 7, and 1 or 8, are used for data communication after a program uploaded to the chip.

3. Fabrication and evaluation of distributed force sensor

3.1. Fabrication of the contact-resistance force sensor

Some researchers have tried to use a flexible PCB in order to place the sensing part and its electric circuit into the curved structure like fingertip. Cannata et al. have proposed a flexible triangular modular robot skin system based on the flexible PCB [31]. Schmitz et al. have reported the fingertip module with above mentioned triangular module in [26]. They showed an effective method in terms of flexibility and optimum use of space. We considered the distributed force sensor with strip-type shape in order to apply to the slots like groove of the fingertip structure that has a small radius curvature and many taxels, if possible. We have also tried to get the small-sized FPCB for the optimum use of space. Thus, we finally designed the FPCB with long signal lines between the sensing part and the electronics as shown in Fig. 3 that can be bended and inserted into the fingernail part of Fig. 2. Fig. 4 describes the fabrication process of the film type contact-resistance force sensor using a silk screen printing technique. The polyimide is well known for its thermal stability, robust chemical resistance, and excellent mechanical properties. The FPCB is made of flexible copper clad laminate (FCCL) with a 54 μm thick polyimide film, whereas that of copper is 11 μm (Fig. 4(a)). The pattern of the contact signal terminal line is made through the etching process (Fig. 4(b)), and conductive and resistive layers are coated using the screen printing

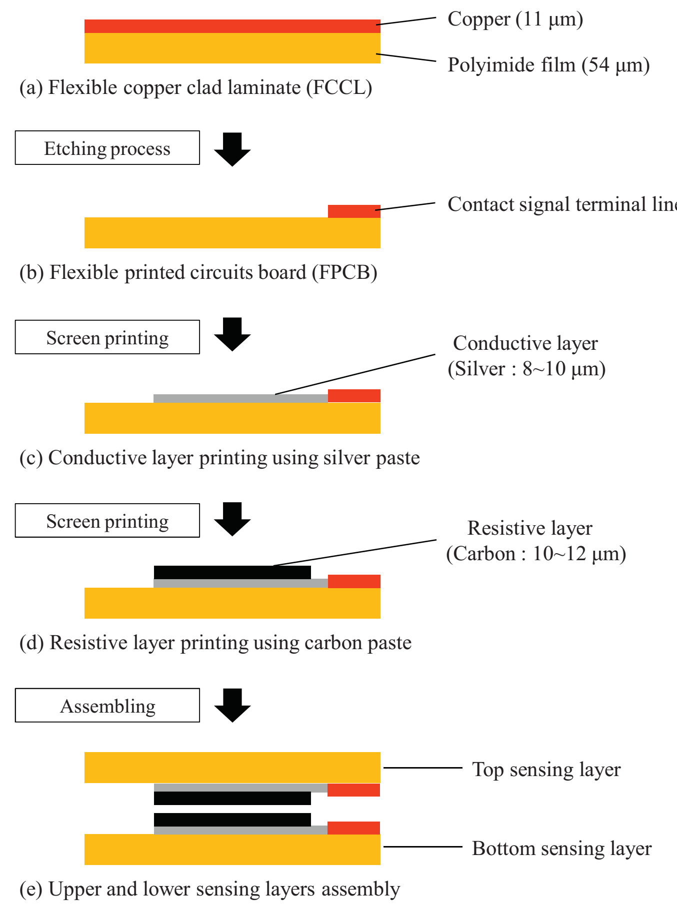

Fig. 4. Five steps for fabrication process of the contact-resistance force sensors using flexible printed circuit board (FPCB) and screen printing technique.

method. We use a high precision semi-automatic printing machine (model LSP-6050L, Linesystem Co.), which uses a square-edge type squeegee made of polyurethane material with shore hardness (Hs) of 70 durometer and is necessary to spread paste onto the screen mask. A conductive layer (Fig. 4(c)) is formed on the film using a silver paste (MISUNG Polytech Co., Ltd.) and a 300-mesh mask. The coated film is leveled at room temperature for 10 min and then cured in an oven at 140 °C for 10 min. A resistive layer is coated (Fig. 4(d)) using carbon paste based on polymer and carbon black (MISUNG Polytech Co., Ltd.) and a 250-mesh mask. These pastes have passed a reliability test (temperature: 70 °C, humidity: 90%, 48 h), so it guarantees durability and performance. The carbon paste is cured in an oven at 150 °C for 60 min after being leveled at room temperature for 10 min. Finally, the upper and lower surfaces of the printed film are assembled together (Fig. 4(e)).

3.2. Fabrication of the force sensing part

Fig. 5 presents the distributed force sensor with a flexible electric circuit board for signal processing. The sensing part has an array of 37 sensing taxels, and each cell is 2 mm in diameter (Fig. 5 (bottom)). The distributed force sensor and signal processing part are neatly integrated onto the same FPCB to apply to the robot fingertip module, except for the four signal lines used to communicate with PC.

We did take into account the total number of ports for the input and output channels of the matrix-type force sensors to select the main electronic, MCU. The number of ports for the input voltage and the output A/D should be more than 7, respectively. The sampling rate of the MCU should be fast, if possible, to obtain a good dynamic

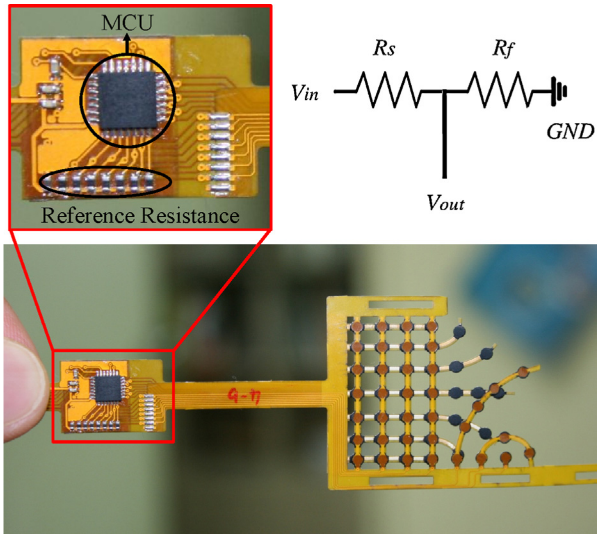

Fig. 5. Photographs of the fabricated sensing part with a flexible electric circuit board for signal processing: (bottom) fabricated sensing part with flex-circuit board; (top left) flexible electric circuit board with micro controller unit (MCU) and reference resistance; (top right) schematic of simple voltage divider circuits.

response. The size should be smaller than 11 mm × 10 mm, the size of the FPCB to insert the components into the fingertip module. The price of a chip should be cheap for the cost-effective fingertip module, if possible. The tiny and cheap commercial signal processing chip was used for signal data acquisition and analog-to-digital conversion (ADC). We used 8-bit ultralow power MCU (model STM8L151G6, ST Microelectronics Co.) with twenty-eight pins. The chip provides 12 bit ADC with up to 1 Msps sampling rate per 25 channels, and standard communication interface such as SPI (Serial Peripheral Interface Bus), I2C (Inter Integrated Circuit), and USART (Universal Synchronous Asynchronous Receiver Transmitter). Fig. 5 (top left) shows the fabricated signal processing board. The contact-resistance force sensor is a variable resistor, with resistance varying from about 1 kΩ up to 100 kΩ under loading force. In addition, the fabricated sensor does not require amplification because of its large changes in resistance by loading force. Thus, resistance was measured by using simple voltage divider circuit (Fig. 5 (top right)), with the reference resistance (R_f) at 500 Ω and the input voltage (V_{in}) is 3.3 V. Output voltage (V_{out}) can be expressed as follows:

$$V_{\text{out}} = \frac{R_f}{R_f + R_s} V_{\text{in}} \quad (1)$$

where R_s is the resistance of the force sensor. Fig. 6 illustrates the schematic diagram of the electrical signal flow from the force sensing element to the computer. The MCU controls the row-direction multiplexing in order to provide the input voltage to the sensor array. Then, the analog output data from the sensing elements are connected to the A/D ports. The digital data are transmitted via USART serial communication interface with 1 Mbps full duplex. A FTDI USB MCU (model FT232RL, FTDI Ltd.) was used for USART-to-USB conversion. Array type tactile sensor usually has crosstalk between adjacent sensing elements because parasitic resistors are present between taxels. Even if the sensor array is composed of discrete taxels in rows and columns, the crosstalk is found in the sensor array [32]. To reduce the interference and solve this crosstalk problem, some researchers have proposed a few strategies such as a grounding method [21,32–34]. We also have tried to reduce crosstalk in our previous MEMS-based tactile sensor array in [35]. However, it is not easy to make the small-sized electronic circuit considering crosstalk error, which needs high-cost fabrication. We simulated the electrical circuit shown

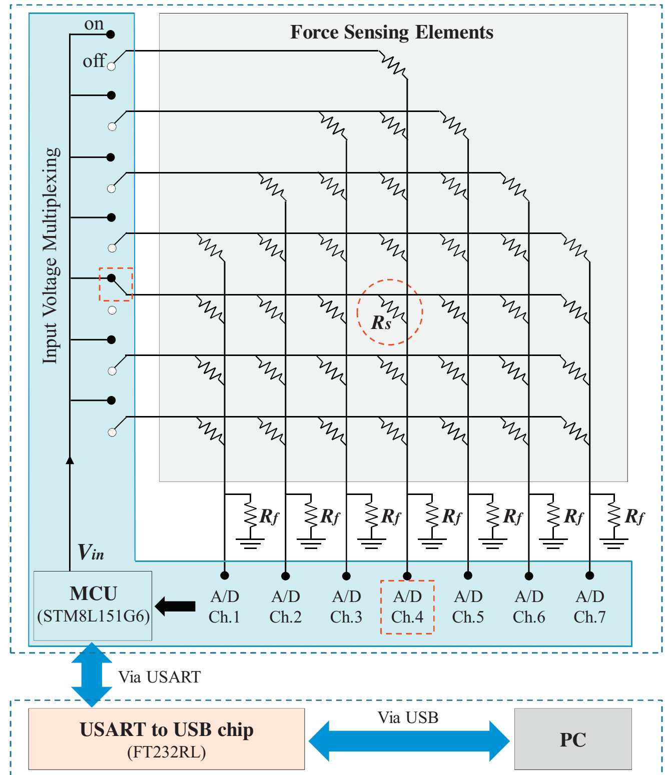

Fig. 6. Electrical schematic diagram of a signal flow from the force sensing element to PC, and functions of each signal processing units.

in Fig. 6 using Schematics® software (Design Lab) to evaluate the crosstalk error when some taxels are pressed simultaneously. We considered some case examples, and obtained that the interference error was below 0.3%. The maximum crosstalk error was about 17% when all taxels are pressed except of R_s within force sensing elements shown in Fig. 6.

3.3. Static and dynamic evaluation of distributed force sensor and its result

We used an evaluation setup to measure each force response of the distributed force sensor under static load. Fig. 7 shows the evaluation setup composed of a multi-component (F_x, F_y, F_z) load-cell and its probe tip, *xyz*-axes positioning stages, and PC. The load-cell (CURIOSITY TECHNOLOGY Co., Ltd. Model CMAS111) has

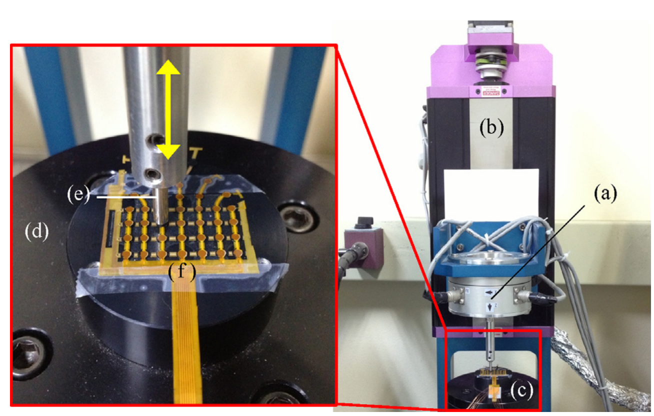

Fig. 7. Evaluation setup to evaluate the force response of the distributed force sensor: (a) three-axis load-cell, (b) *z*-axis linear stage, (c) *x*- and *y*-axes positioning stages, (d) top plate of the stage, (e) ϕ2 probe, and (f) distributed force sensor.

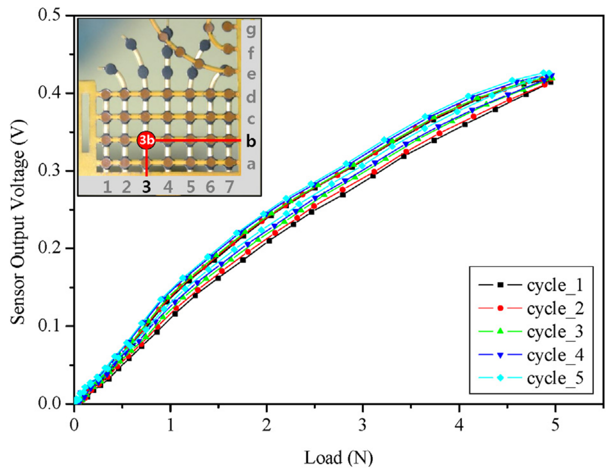

Fig. 8. Output signal of 'taxel 3b' obtained from loading and unloading under five repetitive cycles.

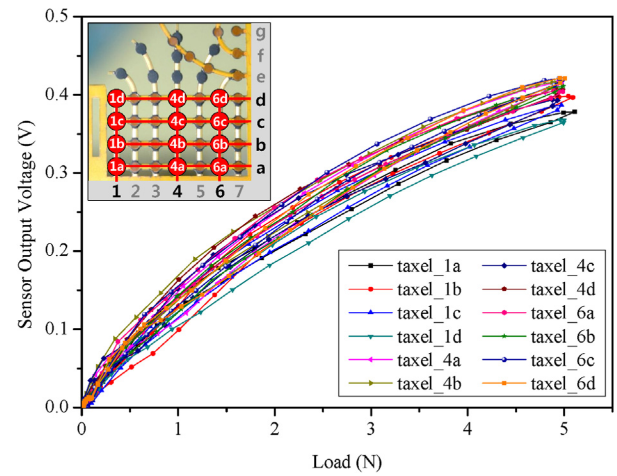

Fig. 9. Output signals of each fifth cycle of twelve taxels obtained from loading and unloading under five repetitive cycles.

a capacity of 10 N in three directions. The *z*-axis linear stage, which has a 1 μm resolution, was used to apply a normal load to one taxel of the distributed force sensor. The *x*- and *y*-axes positioning stages were used to check the alignment between the probe and a target taxel. The cylinder-shape probe tip has the same diameter of 2 mm as the taxel. Analog amplifiers (Instrument Division Co., Model 2210) were used to amplify the output signals of the load-cell. We used the PXI module (National Instrument™): PXI-7340 for motor control and PXI-6221 for signal acquisition of the load-cell. The analog output signal data of the target taxels were also acquired and converted to digital data through the signal processing part. LabVIEW™ was used to control the linear stage and obtain data from the distributed force sensor and the load-cell.

Fig. 8 presents the force response of the 'taxel 3b' during five repetitive cycles. The '3b' means a 'column 3' and 'row b'. The force response was obtained by loading and unloading conditions from 0 N to 5 N. Five repetitive cycles were carried out to check repeatability. The target taxel was aligned by the *x*- and *y*-axes positioning stages. The *z*-axis linear stage moves at a speed of 0.5 mm/min. The sensor has a hysteresis error of 8.2% and a repeatability error of 4.5% with respect to the full scale (5 N). Threshold sensitivity of the force sensor is about 0.1 N. On the other hand, twelve taxels, each four cells on the columns 1, 4, and 6, were chosen to evaluate the uniformity error of the distributed force sensor. Taxels from the row 'e' to 'g' are not available for evaluation because the top layer and the bottom layer cannot be aligned due to 3D-curved shape of the module. Each taxel was evaluated five times under above conditions; 0 N to 5 N force range and 0.5 mm/min moving speed. Fig. 9 shows the force response corresponding to each fifth cycle obtained from twelve taxels. The taxel to taxel maximum error is about ±9.5% with respect to the full scale. Fig. 10 shows the impulse loading setup to obtain the dynamic response of the force sensor. The impulse loading of 0.5 N was applied to the surface of the 'taxel 4d'. Output signal was measured by a dynamic signal analyzer (Agilent Technologies, Inc., Model 35670A) using simple voltage divider circuit. The reference resistance is 500 Ω, and the input voltage is 3.3 V. Fig. 10 also shows the good dynamic response during 40 ms after impulse loading. Sampling rate of analyzer is about 0.25 ms, and the rise and fall times are about 2 ms, respectively.

3.4. Fatigue test of distributed force sensor and its results

Fig. 11 shows the high-cycle fatigue test setup composed of an electro-dynamic type actuator, a power amplifier, and a load-cell [36]. The load-cell based on strain-gage has a capacity of 50 N. Analog amplifier (Instrument Division Co., Model 2210) was used to amplify the output signals of the load-cell. The electro-dynamic type actuator based on speaker principle consists of a field magnet and the moving bobbin with coil. Also, a linear guide is used to prevent the bobbin with coil from vibrating horizontally. The electro-dynamic type actuator can produce up to 100 Hz in the range of 50 N. We used the PXI module (National Instrument™): PXI-8106 embedded controller for system control and data processing, and PXI-6221 for signal acquisition of load-cell and force sensor. Output voltages of the taxel were measured by the simple voltage-divider-circuit board as shown in Eq. (1); input voltage was 3.3 V and the reference resistance was 500 Ω. The acquisition of data and its analysis was performed automatically by LabVIEW™.

There are three typical fatigue test cycles: a fully reversed loading cycle, a repeated offset loading cycle, and a random loading

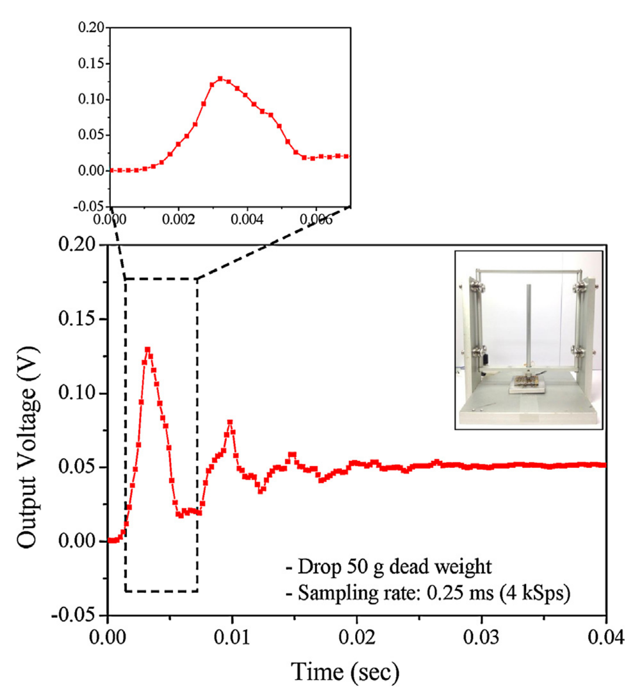

Fig. 10. Dynamic response of the contact-resistance force sensor at 'taxel 4d' after an impulse loading test with 50 g dead weight.

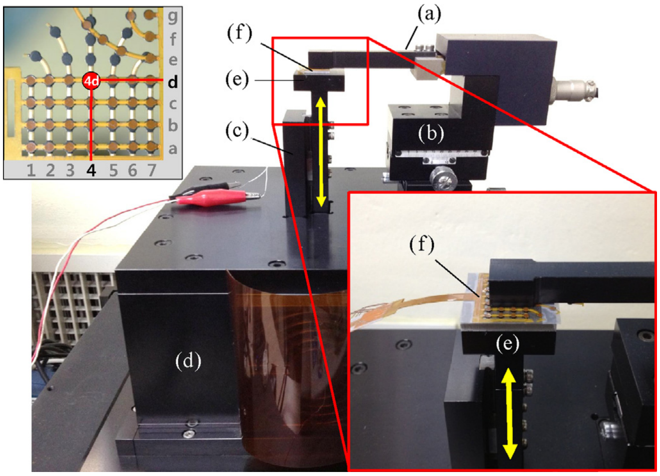

Fig. 11. Fatigue test setup with moving coil linear stage to evaluate the durability of the sensor: (a) cantilever type load-cell, (b) positioning stage, (c) linear-guide, (d) actuator part composed of field magnet and moving bobbin with coil, (e) jig and flat plate, and (f) distributed force sensor.

cycle [37]. We employed the repeated offset loading cycle for the high-cycle fatigue test. The distributed force sensor was evaluated by moving the jig at a speed of 10 Hz as the sine waves. The sine wave has peak (5 N) and valley (0.5 N), and the output signals of load-cell and the target taxel were acquired at the sampling rate of 10 kHz. Each peak and valley signal of both the load-cell and the taxel were measured during 10^6 loading cycles. Fig. 12 shows fatigue test results of the 'taxel 4d'. An average of the output voltage was 0.056 V at the minimum load 0.5 N, and was 0.34 V at the 5 N. Sensor output voltages increased by 0.005 V during after 10^6 cycles. The fatigue test presents that the fabricated sensor is durable and robust.

4. Fabrication and evaluation of robot fingertip module

4.1. Fabrication of fingertip structure using molding technique

In general, it is important to cut down the manufacture cost of robot components in order to commercialize a robot product. Thus we adopted the molding technique known as an effective method for mass production. Especially, in case of mass production of a 3D-curved structure, it is not easy to cut down the cost using a general manufacture technique. Fig. 13(a) shows the aluminum molds for fingertip structures: the left is for the inside part and the right is for

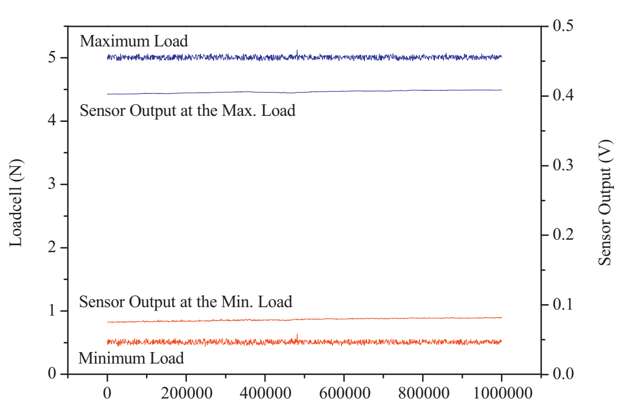

Fig. 12. Output signals of 'taxel 4d' obtained from a fatigue test with sine wave of 10 Hz, and the range of force is from 0.5 N to 5 N.

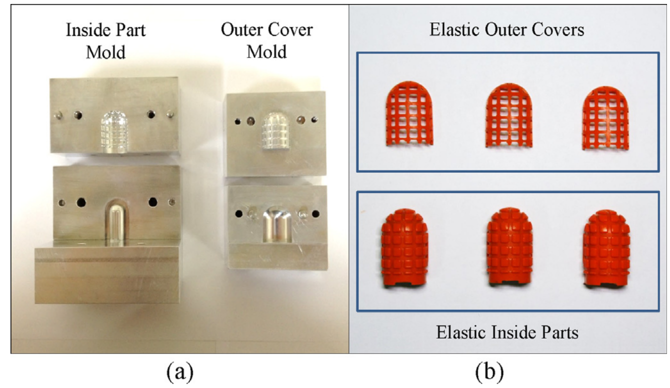

Fig. 13. Photographs of molds and the molded fingertip structures: (a) aluminum molds for the elastic inside parts and the outer cover, (b) the manufactured outer cover products and elastic inside part products.

the outer cover. We used a vinyl-poly-siloxane (HANDAE Chemical Co., Ltd.) as an inserting material of the inside part and the outer cover because of its low curing temperature (about 10–40 °C) and short curing time (5–20 min). Fig. 13(b) presents the molded fingertip structures. The manufactured elastic inside part and the outer cover have a human-like soft texture and a curved surface. Fig. 14(a) presents that the sensor and the signal processing circuits are neatly inserted into the fingertip structure. Only four signal lines are used to communicate with PC. Fig. 14(b) shows the assembled module of the fabricated fingertip structures and the distributed force sensor. The module is 16.3 mm in depth, 16.6 mm in length, and 38 mm in height. On the other hand, Fig. 14(c) represents the fabricated module integrated with a dummy hand. It also shows that the fingertip tactile sensing module can be replaceable easily when the fingertip module breaks down.

4.2. Static and dynamic evaluation of assembled module and its result

We also used the evaluation setup shown in Fig. 7 to evaluate the force response of the assembled fingertip tactile sensing module. Two types of swing-jig were fabricated to roll and pitch the fingertip module. It is important to apply exactly a normal load to the target taxel of 3D-curved fingertip structure. Fig. 15 shows the evaluation setup and two types of swing-jig. The force response was performed under static load condition. The module was evaluated from the vertical movements of the z-axis linear stage. The force response of the module was measured at one point, taxel 4c. The load range is from 0 N to 5 N under loading and unloading conditions. Five

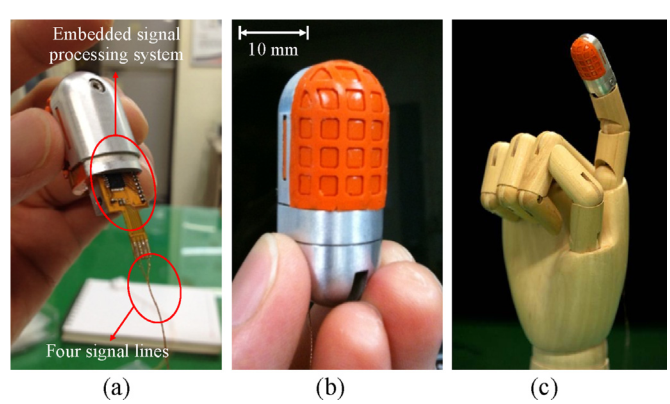

Fig. 14. Photographs of the assembled robot fingertip tactile sensing module: (a) built-in sensor and signal processing system with four signal lines; (b) fingertip module; (c) module assembled with dummy hand.

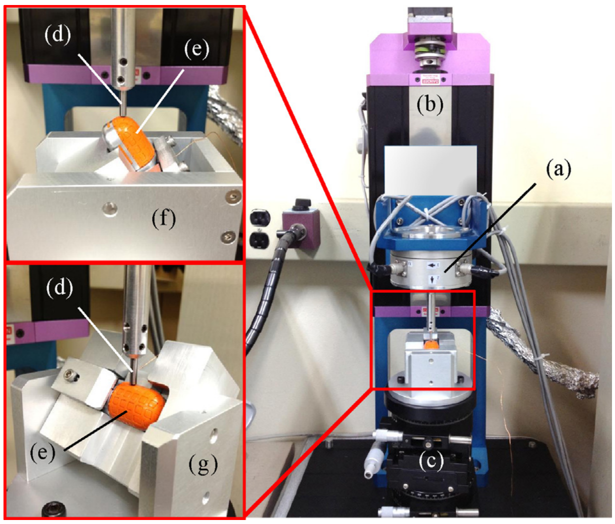

Fig. 15. Evaluation setup to evaluate the assembled robot fingertip tactile sensing module with two types of swing-jig: (a) three-axis load-cell, (b) z-axis linear stage, (c) x- and y-axes positioning stage, (d) ϕ2 probe, (e) robot fingertip tactile sensing module, (f) swing jig for vertical rotation, and (g) swing jig for horizontal rotation.

repetitive cycles were carried out to check repeatability. Fig. 16 presents the force response of the 'taxel 4c' during five repetitive cycles. The hysteresis error and the repeatability error are about 9.3% and 5% with respect to the full scale (5 N), respectively. The repeatability error of the module is almost the same as that of the distributed force sensor. The hysteresis error is about 0.5% higher and the repeatability error is about 0.9% higher than that of the distributed force sensor.

On the other hand, it is very useful to obtain the contact information and force response at tip and side-edge areas of the fingertip in case of the grasping task. Thus, we selected and evaluated all taxels on 'column 4'. The module was loaded on each swing-jig, and the target taxel was aligned by the x- and y-axes positioning stages. Then, we had the z-axis linear stage moves at a speed of 0.5 mm/min until the load reaches 5 N. We removed the load at the same speed. Each taxel was evaluated five times under the same conditions. Fig. 17(a) shows each fifth cycle of the seven taxels on the 'column 4'. The taxel to taxel maximum error is about ±10.3%

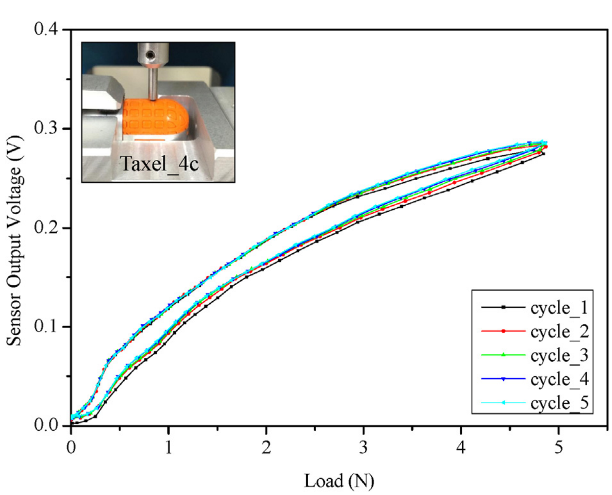

Fig. 16. Output signal of 'taxel 4c' obtained from loading and unloading during five repetitive cycles.

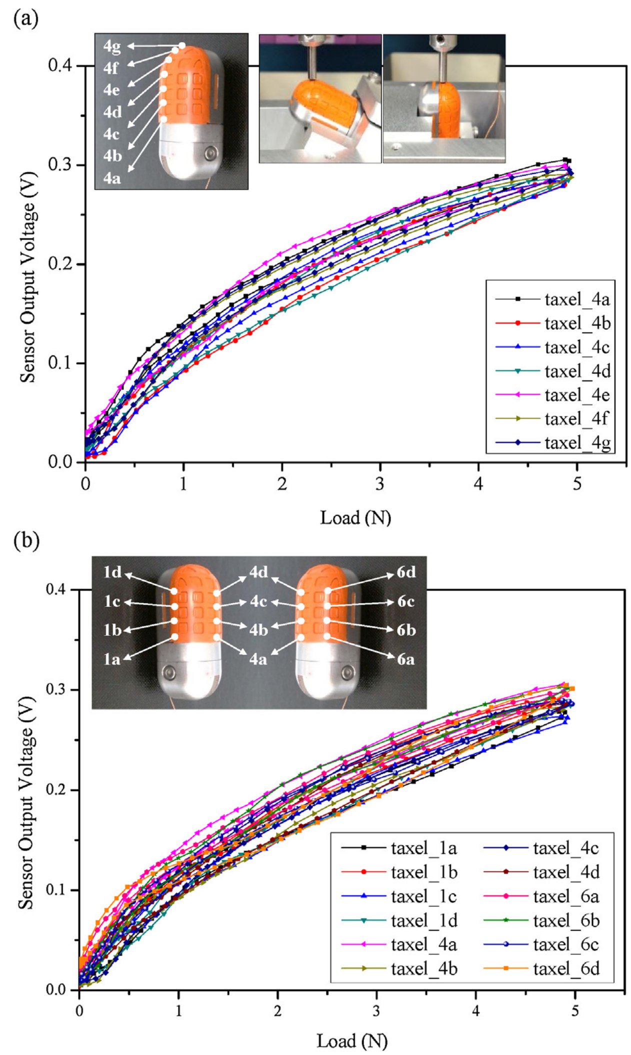

Fig. 17. Output signal of each fifth cycle obtained from loading and unloading: (a) force response graphs of seven taxels on the 'column 4', and (b) force response graphs of twelve taxels on the 'column 1, 4, and 6'.

with respect to the full scale. The average output voltage of the distributed force sensor at the maximum load (5 N) was about 0.4 V, whereas that of the module is about 0.3 V. When the elastic outer cover was inserted into the slot of the elastic inside parts, the friction between two structures was occurred due to the inaccurate size of the molded structures compared to its design size. Thus the normal load was not fully applied to the distributed force sensor. Threshold sensitivity of the assembled tactile sensing module is about 0.2 N, which was larger than 0.1 N of the distributed force sensor. It was also caused by the geometry of the molded two structures. Fig. 17(b) shows each fifth cycle of the twelve taxels on the 'columns 1, 4, and 6'. The taxel to taxel maximum error was ±10% similar to that of the Fig. 17(a). Meanwhile, the dynamic response test was performed to know the temporal behavior of the assembled fingertip module with its signal processing part. Fig. 18 shows that an impulse loading of 0.5 N was applied to the 'taxel 1c' through the impulse loading setup. Output signal was measured by a signal processing part with MCU, and the data were transmitted to the computer via USART serial communication interface. Fig. 18 also shows the impulse response during 40 ms after the impulse loading. Sampling rate of the module was measured as about 2 ms. The dynamic response has similar behavior compared to the force sensor.

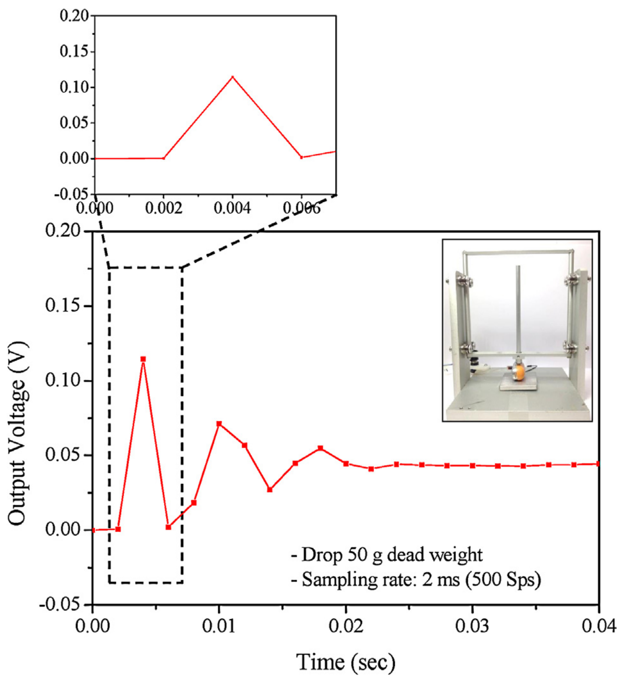

Fig. 18. Dynamic response of 'taxel 1c' of the robotic fingertip module after an impulse loading test with 50 g dead weight.

5. Conclusions and future work

In this paper, we have proposed a compact and replaceable robot fingertip tactile sensing module and its simple production method. The fabricated module has a human fingertip-like 3D-curved shape and its radius of curvature is about 7 mm. A spatial resolution of the module is about 4 mm. The module can detect both contact force and location simultaneously. The force threshold sensitivity of an assembled module is about 0.2 N. We suggested the fabrication technique that apply 2D-type distributed force sensor to 3D-curved fingertip structure. The distributed force sensor has a strip-type structure. The fingertip structure was fabricated easily by molding technique. The assemble method can be employed not only to the robot fingertip but also to various curved structure of robot such as head, arm, shoulder, etc. The developed sensing module is compact and replaceable. Its fabrication process is also simple and low-cost, which can be applicable to mass production.

In our follow-up study, we will collaborate with Korea Institute of Science and Technology (KIST) to integrate our tactile sensing module into a home service robot platform, CIROS [38], for the grasping and manipulation tasks. We also have a plan to apply our fabrication technique to the curved body of an English teaching robot platform, ENGKEY [39], for the purpose of human–robot interaction.

Acknowledgement

This work was supported by the Industrial Strategic Technology Development Program (10041066, Development of tactile information storing and playing platform based on flexible sensors for immersible media) funded by the Ministry of Knowledge Economy (MKE, Korea).

References

[1] A. Austermann, S. Yamada, Teaching a pet-robot to understand user feedback through interactive virtual training tasks, J. Auton. Agent Multi-Agent Syst. 20 (2010) 85–104.
[2] H. Iwata, S. Sugano, Human–robot-contact-state identification based on tactile recognition, IEEE Trans. Ind. Elect. 52 (2005) 1468–1477.
[3] R.S. Dahiya, M. Valle, Robotics Tactile Sensing – Technologies and System, Springer, 2013, ISBN: 978-94-007-0578-4.
[4] R.S. Dahiya, G. Metta, M. Valle, G. Sandini, Tactile sensing-from humans to humanoids, IEEE Trans. Robot. 26 (2010) 1–20.
[5] M.I. Tiwana, S.J. Redmond, N.H. Lovell, A review of tactile sensing technologies with applications in biomedical engineering, Sens. Actuators A 179 (2012) 17–31.
[6] M.E.H. Eltaib, J.R. Hewit, Tactile sensing technology for minimal access surgery, Mechatronics 13 (2003) 1163–1177.
[7] B.D. Argall, A.G. Billard, A survey of tactile human–robot interactions, Robot. Auton. Syst. 58 (2010) 1159–1176.
[8] H. Yousef, M. Boukallel, K. Althoefer, Tactile sensing for dexterous in-hand manipulation in robotics – a review, Sens. Actuators A 167 (2011) 171–187.
[9] G. Kinoshita, S. Aida, M. Mori, Pattern recognition by an artificial tactile sense, in: Proceedings of the 2nd International Joint Conference on Robots and Integrated Systems Session No. 8, 1971, pp. 376–384.
[10] T. Mouri, H. kawasaki, K. Yoshikawa, J. Takai, S. Ito, Anthropomorphic robot hand: Gifu Hand III, in: Proceedings of the International Conference on Control, Automation and Systems, Jeonbuk, Korea, 2002, 1288-1293.
[11] H. Zhang, E. So, Hybrid resistive tactile sensing, IEEE Trans. Syst. Man Cybern. B Cybern. 32 (2002) 57–65.
[12] J.H. Kim, J.I. Lee, H.J. Lee, Y.K. Park, M.S. Kim, D.I. Kang, Design of flexible tactile sensor based on three-component force and its fabrication, in: Proceedings of the IEEE Conference on Robotics and Automation, 2005, pp. 2578–2581.
[13] D.K. Kim, J.H. Kim, H.J. Kwon, Y.H. Kwon, Fabrication of robot head module using contact-resistance force sensor for human–robot interaction and its evaluation, J. Mech. Sci. Technol. 26 (2012) 3269–3276.
[14] F. Castelli, An integrated tactile-thermal robot sensor with capacitive tactile array, IEEE Trans. Ind. Appl. 38 (2002) 85–90.
[15] H.K.S.G.L. Kim, K.S. Yun, Capacitive tactile sensor array for touch screen application, Sens. Actuators A 165 (2011) 2–7.
[16] J. Castellanos-Ramos, R. Navas-Gonzalez, H. Macicior, T. Sikora, E. Ochoteco, F. Vidal-Verdu, Tactile sensors based on conductive polymers, Microsyst. Technol. 16 (2010) 765–776.
[17] R.S. Dahiya, G. Metta, M. Valle, L. Lorenzelli, A. Adami, Piezoelectric oxide semiconductor field effect transistor touch sensing devices, Appl. Phys. Lett. 95 (2009).
[18] R.S. Dahiya, D. Cattin, A. Adami, C. Collini, L. Barboni, M. Valle, L. Lorenzelli, R. Oboe, G. Metta, F. Brunetti, Towards tactile sensing system on chip for robotic applications, IEEE Sens. J. 11 (2011) 3216–3226.
[19] J. Jockusch, J. Walter, H. Ritter, A tactile sensor system for a three-fingered robot manipulator, in: Proceedings of the IEEE International Conference on Robotics and Automation, Albuquerque, New Mexico, April, 1997, pp. 3080–3086.
[20] Y.J. Yang, M.Y. Cheng, W.Y. Chang, L.C. Taso, S.A. Yang, W.P. Shih, F.Y. Chang, K.C. Fan, An integrated flexible temperature and tactile sensing array using PI-copper films, Sens. Actuators A 143 (2008) 143–153.
[21] Tekscan, http://www.tekscan.com/products3
[22] FSR, http://www.interlinkelectronics.com
[23] D.K. Kim, J.H. Kim, Y.K. Park, Y.H. Kwon, Robot Fingertip Module for Measuring Contact Force and Location, in: Proceedings of the XX IMEKO World Congress, Busan, Republic of Korea, 2012 http://www.imeko.org/publications/wc-2012/IMEKO-WC-2012-TC17-O5.pdf
[24] R. Andrew Russell, Robot Tactile Sensing, Prentice Hall, Inc., 1990, pp. 135–139 (ch.9).
[25] J.H. Kim, M.S. Kim, Y.K. Park, D.I. Kang, D.K. Kim, Structure and method for attaching tactile sensor to curved surface, US Patent Appl. No. 13/421945, March 16 (2012).
[26] A. Schmitz, P. Maiolino, M. Maggiali, L. Natale, G. Cannata, G. Metta, Methods and technologies for the implementation of large scale robot tactile sensors, IEEE Trans. Robot. 27 (2011) 389–400.
[27] BioTAC, http://www.syntouchllc.com/Home/Homepage.php
[28] N. Wettels, V.J. Santos, R.S. Johansson, G.E. Loeb, Biomimetic tactile sensor array, Advanced Robotics 22 (2008) 829–849.
[29] J.H. Kim, H.J. Kwon, Y.K. Park, M.S. Kim, D.I. Kang, J.H. Choi, Tactile sensor for curved surface and manufacturing method thereof. US Patent No. 8049591, November 1 (2011).
[30] R. Andrew Russell, Robot Tactile Sensing, Prentice Hall, Inc., 1990, pp. 48 (ch. 5).
[31] G. Cannata, R. Dahiya, M. Maggiali, F. Mastrogiovanni, G. Metta, M. Valle, Modular skin for humanoid robot systems, in: Proceedings of the 4th International Conference on Cognitive Systems (CogSys 2010), 2010.
[32] D. Goger, H. Worn, A highly versatile and robust tactile sensing system, in: Proceedings of the 2007 IEEE International Conference on Sensors, 2007 October, pp. 1056–1059.
[33] F. Vidal-Verdu, O. Oballe-Peinado, J.A. Sanchez-Duran, J. Castellanos-Ramos, R. Navas-Gonzalez, Three realizations and comparison of hardware for piezoresistive tactile sensors, Sensors 11 (2011) 3249–3266.
[34] M. Shimojo, A. Namiki, M. Ishikawa, R. Makino, K. Mabuchi, A tactile sensor sheet using pressure conductive rubber with electrical-wires stitched method, IEEE Sens. J. 4 (2004) 589–596.
[35] J.H. Kim, W.C. Choi, H.J. Kwon, D.I. Kang, Development of tactile sensor with functions of contact force and thermal sensing for attaching to intelligent robot

finger tip, in: Proceedings of 2006 IEEE International Conference on Sensors, 2006 October, pp. 22–25.
[36] J.H. Song, Y.S. Shin, Y.S. Im, Construction of small-sized, electro-dynamic type bending fatigue testing machine, Trans. KSME A 13 (1989) 199–201.
[37] F.C. Campbell, Elements of Metallurgy and Engineering Alloys, ASM International, Materials Park, OH, 2008, pp. 243–264.
[38] CIROS, http://www.irobotics.re.kr/eng_sub1_3
[39] ENGKEY, http://www.irobotics.re.kr/eng_sub1_1

Biographies

Dong-Ki Kim received his B.S. and M.S. degrees in Mechanical Engineering from Kyung Hee University, Yongin, Gyunggi-Do, Republic of Korea in 2008 and 2010, respectively. Since 2010, as a temporary position, he has been with the Korea Research Institute of Standards and Science (KRISS), Daejeon, Republic of Korea. His current research interests include design and fabrication of tactile sensor for input device and robots.

Jong-Ho Kim received his B.S. degree in Mechanical Engineering from Kyungpook National University, Daegu, Korea in 1992. He received his M.S. and Ph.D. degrees in Mechanical Engineering from the Korea Advanced Institute of Science and Technology (KAIST), Daejeon, Republic of Korea in 1994 and 2001, respectively. Since 2001, he has been with the Korea Research Institute of Standards and Science (KRISS). His current research interests include the development of tactile sensor/actuator, its fabrication, and application.

Young-Tae Kim received his B.S. degrees in Mechanical Engineering from Kyung Hee University in 2012. He is currently pursuing his M.S. degree in Mechanical Engineering from Kyung Hee University, Yongin, Gyunggi-Do, Republic of Korea. Since 2012, as a student position, he has been with the Korea Research Institute of Standards and Science (KRISS), Daejeon, Republic of Korea. His current research interests include design and fabrication of touch sensor and actuator.

Min-Seok Kim received his B.S. degree in Mechanical Engineering from the Korea Advanced Institute of Science and Technology (KAIST), Daejeon, Korea in 1996. He also received his M.S. and Ph.D. degrees in Mechanical Engineering from KAIST, in 1998 and 2002, respectively. Since 2002, he has been with the Korea Research Institute of Standards and Science (KRISS). His current research interests include the development of tactile sensor, its fabrication, and torque measurement.

Yon-Kyu Park received his B.S. degree in Mechanical Engineering from the Korea Advanced Institute of Science and Technology (KAIST), Daejeon, Korea in 1991. He also received his M.S. and Ph.D. degrees in Mechanical Engineering from KAIST, in 1993 and 1998, respectively. Since 1998, he has been with the Korea Research Institute of Standards and Science (KRISS). His current research interests include the development of tactile sensor, its fabrication, and force measurement.

Young-Ha Kwon received his B.S degree in Textile Engineering from Kyung-Hee University, Yongin, Republic of Korea, in 1982. He received his M.S and Ph.D. degrees in Mechanical Engineering, from University of Illinois at Chicago, Chicago, USA, in 1984 and 1987, respectively. Since 1992, as a professor, he has been with Kyung-Hee University, Yongin, Republic of Korea. His current research interests include the characteristic of human's skin and its application.